

ROCK Controls Matrix Synthesis in Vascular Smooth Muscle Cells

Coupling Vasoconstriction to Vascular Remodeling

Rene Chapados, Khotaro Abe, Kaori Ihida-Stansbury, David McKean, Adam T. Gates, Michael Kern, Sandra Merklinger, John Elliott, Anne Plant, Hiroaki Shimokawa, Peter Lloyd Jones

Abstract—Tenascin-C (TN-C) is an extracellular matrix (ECM) protein expressed within remodeling systemic and pulmonary arteries (PAs), where it supports vascular smooth muscle cell (SMC) proliferation. Previously, we showed that A10 SMCs cultivated on native type I collagen possess a spindle-shaped morphology and do not express TN-C, whereas those on denatured collagen possess a well-defined F-actin stress fiber network, a spread morphology, and they do express TN-C. To determine whether changes in cytoskeletal architecture control TN-C, SMCs on denatured collagen were treated with cytochalasin D, which decreased SMC spreading and activation of extracellular signal-regulated kinase 1/2 (ERK1/2), signaling effectors required for TN-C transcription. Next, to determine whether cell shape, dictated by the F-actin cytoskeleton, regulates TN-C, different geometries of SMCs (ranging from spread to round) were engineered on denatured collagen: as SMCs progressively rounded, ERK1/2 activity and TN-C transcription declined. Because RhoA and Rho kinase (ROCK) regulate cell morphology by controlling cytoskeletal architecture, we reasoned that these factors might also regulate TN-C. Indeed, SMCs on denatured collagen possessed higher levels of RhoA activity than those on native collagen, and blocking RhoA or ROCK activities attenuated SMC spreading, ERK1/2 activity, and TN-C expression in SMCs on denatured collagen. Thus, ROCK controls the configuration of the F-actin cytoskeleton and SMC shape in a manner that is permissive for ERK1/2-dependent production of TN-C. Finally, we showed that inhibition of ROCK activity suppresses SMC TN-C expression and disease progression in hypertensive rat PAs. Thus, in addition to its role in regulating vasoconstriction, ROCK also controls matrix production. (*Circ Res.* 2006;99:837-844.)

Key Words: tenascin-C ■ smooth muscle ■ ROCK ■ pulmonary hypertension

Adult vascular smooth muscle cells (SMCs) reside within a type I collagen-enriched extracellular matrix (ECM) that helps to maintain the majority of these cells in a nonmotile, growth-arrested, and differentiated state.¹⁻⁴ Following vascular injury, however, ECM-degrading matrix metalloproteinases (MMPs) remodel the preexisting ECM to create a tissue microenvironment that is conducive for SMC proliferation, migration, and survival.³⁻⁵ Understanding how alterations in adhesive interactions within the vascular ECM modify SMC behavior, therefore, represents an important question in vascular pathobiology.

Tenascin-C (TN-C) is an ECM glycoprotein induced within remodeling hypertensive pulmonary arteries (PAs),⁶⁻¹⁰ as well as in systemic, obliterative vasculopathies,¹¹⁻¹³ where it supports vascular SMC proliferation, migration, and sur-

vival.^{4,14,15} In keeping with the idea that TN-C plays a direct role in promoting vascular disease, studies using TN-C null mice demonstrate that these animals are refractory to neointimal hyperplasia after aortotomy.¹¹ Further, blocking TN-C expression in cultured hypertensive rat PAs induces regression of vascular lesions.¹⁶ As well, radiolabeled TN-C antibodies have been used in clinical trials to stabilize the progression of malignant glioma and non-Hodgkins lymphoma,^{17,18} and increased circulating levels of TN-C are associated with ongoing fibrosis in patients with idiopathic dilated cardiomyopathy.¹⁹

Given these therapeutic and diagnostic roles for TN-C in vascular pathobiology, investigations have been made to determine how this protein is regulated, and in this regard, activated MMPs have been shown to promote TN-C expres-

Original received September 2, 2004; resubmission received June 20, 2006; revised resubmission received September 3, 2006; accepted September 8, 2006.

From the Children's Hospital of Philadelphia (R.C., A.T.G.), Pa; Kyushu University Graduate School of Medical Sciences (K.A., H.S.), Fukuoka, Japan; The Institute for Medicine and Engineering (K.I.-S., P.L.J.) and the Department of Pathology and Laboratory Medicine (P.L.J.), University of Pennsylvania, Philadelphia; Department of Pediatrics (D.M.), University of Colorado Health Sciences Center, Denver; Department of Anatomy (M.K.), Medical University of South Carolina, Charleston; The Hospital for Sick Children (S.M.), Toronto, Ontario, Canada; and National Institute of Standards and Technology (J.E., A.P.), Gaithersburg, Md.

Correspondence to Peter Lloyd Jones, PhD, University of Pennsylvania School of Medicine, Institute for Medicine & Engineering, 1010 Vagelos Research Laboratories, 3340 Smith Walk, Philadelphia, PA 19104-6383. E-mail jonespl@mail.med.upenn.edu

© 2006 American Heart Association, Inc.

Circulation Research is available at <http://circres.ahajournals.org>

DOI: 10.1161/01.RES.0000246172.77441.f1

sion.^{4,14,16} For example, pharmacological blockade of MMP activity in cultured PA SMCs and in monocrotaline (MCT)-induced hypertensive PAs suppresses TN-C expression, an event associated with the onset of apoptosis and regression of pulmonary vascular lesions.^{4,14,16} This pathway is not restricted to only PA SMCs, because MMPs also control TN-C expression in calcifying vascular tissues²⁰ and in the tumor stroma associated with experimental breast cancer.²¹ Collectively, these studies indicate that MMPs lie upstream in an adhesion-dependent signaling pathway that regulates TN-C. Consistent with this, cultivating PA or aortic vascular SMCs on native fibrillar type I collagen (an $\alpha_2\beta_1$ integrin ligand) suppresses TN-C, whereas culturing these same cells on MMP-proteolyzed or monomeric/denatured type I collagen (an $\alpha_v\beta_3$ integrin ligand) induces TN-C transcription.²² Mechanistically, SMC interactions with denatured collagen activate an extracellular signal-regulated kinase 1/2 (ERK1/2) mitogen-activated protein kinase (MAPK) signaling pathway that is essential for TN-C gene transcription.²²

Coinciding with the appearance of TN-C in SMCs cultivated on denatured collagen, SMCs also undergo dramatic changes in cell shape, reflecting changes in cytoskeletal organization.⁷ Because RhoA and the Rho kinase-dependent kinase (ROCK) control cytoskeletal architecture,^{23,24} we determined whether RhoA and/or ROCK regulate TN-C expression in isolated vascular SMCs, as well as in a rat model of vascular disease. Our data reveal that TN-C expression is dependent on RhoA and ROCK. Because these mediators also regulate vasoconstriction in pulmonary hypertension,²⁵ our study indicates that vasoconstriction and ECM remodeling in pulmonary hypertension may be coupled via RhoA and ROCK.

Materials and Methods

Animals

Lungs were harvested from adult rats 21 days after injection of MCT or saline. For fasudil experiments, rats were injected with MCT, with or without oral treatment of fasudil, a ROCK inhibitor.²⁶

Immunohistochemistry

Anti-TN-C antibody was applied to 7- μ m lung tissue sections, and detection was achieved using horseradish peroxidase (HRP)-conjugated antibodies. To visualize TN-C, sections were exposed to diaminobenzidine (DAB), before counterstaining with hematoxylin.

Cell Culture

A10 and PA SMCs were maintained in medium 199 (M-199) containing 10% FBS. TN-C promoter activity was measured in TN1/green fluorescent protein (TN1-GFP) SMCs. Native and denatured type I collagen substrates were prepared as described.²⁷ For inhibition of F-actin polymerization, SMCs were treated with 1 μ mol/L cytochalasin D (CCD) or with DMSO. For inhibition of MEK1 or ROCK, cultures were treated with 50 μ mol/L PD98059 (DMSO control) or 30 μ mol/L Y27632 (H₂O control), respectively. For experiments, cells were in M-199 plus 2% FBS.

Immuno- and Cytochemistry

For detection of F-actin, TN-C, and ERK1/2, A10 SMCs were fixed in paraformaldehyde/PBS, permeabilized with Triton-X 100, and blocked in PBS containing BSA and 10% normal goat serum. Cells were incubated either with polyclonal antisera against TN-C (Chemicon), activated ERK1/2 (Cell Signaling), or with a mouse monoclonal antibody against human c-myc (Sigma). Cells were incubated

with a fluorescein isothiocyanate (FITC)-conjugated goat anti-rabbit IgG. For F-actin, cells were stained with AlexaFluor 594 phalloidin. Slides were mounted using Antifade containing 4',6-diamidino-2-phenylindole (DAPI). Photomicrographs were obtained using epifluorescence.

Semiquantitative and Competitive RT-PCR

Semiquantitative RT-PCRs involved these primers: TN-C (forward, 5'-GCTCTCGATGGTCCATCTGGC-3'; reverse, 5'-TCGTAGCA-GTGGTAGAACTC-3'), Prx2 (forward, 5'-ATGGCAGTGCCA-AACGG-3'; reverse 5'-GTTGCAGGACTTGAACCTCC-3'), and GAPDH (forward, 5'-TGGGGCCAAAAGGGTCATCATCTC-3'; reverse, 5'-GCCGCCTGCTTACCACCTTCTT-3'). For competitive PCR, an internal competitor Prx2 cDNA was generated that was smaller from the full-length Prx2. The following primers were used for Prx2: forward, 5'-GGA ATT CGA CAG CGC GGC CGC CGC CTT-3'; reverse, 5'-AGG ACT TGA ACC TCC ACT TGA GCA GCG AGG CAG AGC-3'. The concentration of decoy was adjusted to 100 ng/mL and serially diluted to produce a range of DNA concentrations (10^{-1} to 10^{-10}). Decoy was then added to a known amount (2.5 ng/mL) of cDNA. Final PCR reactions were performed using primers designed for the semiquantitative PCR studies.

Western Immunoblotting

SMCs were lysed, and equal amounts of protein were separated via SDS-PAGE. Proteins transferred to polyvinylidene difluoride (PVDF) membranes were blocked in wash buffer containing 5% nonfat milk. Membranes were incubated either with a rabbit polyclonal anti-TN-C antibody, an anti-GFP mouse monoclonal antibody, or polyclonal antibodies against total or activated ERK1/2. Antigens were visualized by ECL.

Cell SHAPE Analysis

A10 SMCs were permeabilized and stained with Texas Red maleimide. Samples were imaged on a Zeiss Axiovert S100 TV inverted microscope. An outline of each cell was drawn using InnoVision image processing software, and shape was analyzed through the SHAPE module of the software package. Total area was then determined.

Poly-HEME Experiments

Poly-HEME was dissolved in 95% vol/vol ethanol to give final concentrations of 0.05, 0.10, 0.15, 0.20, and 0.25 mg/mL. Before plating poly-HEME, tissue culture plates were precoated with denatured collagen. Surfaces were equilibrated for 3 hours with serum free M-199, before plating and culturing cells for 24 hours.

Rho Pulldown Assays

A10 SMCs were lysed in 1 \times MLB buffer (Upstate Biotechnology), before being centrifuged at 14 000g for 5 minutes. Protein (20 μ g) was analyzed via Western immunoblotting for total RhoA using standard techniques (antibody from Santa Cruz Biotechnology). In parallel, 300 μ g of MLB lysates in 0.5 mL was treated with 40 μ L of Rhotekin RBD-agarose beads (Upstate Biotechnology). After 45 minutes of incubation at 4°C, beads were collected by centrifugation, washed, and resuspended in 2 \times Laemmli buffer. RhoA levels were assessed by Western immunoblotting.

Transfection Studies

Transfection experiments were performed using pcDNA3.1(-)/RhoA-N19-myc as described.²² A10 cells were replated at 48 hours posttransfection onto denatured collagen substrates, before fixation and evaluation of c-myc, TN-C, and F-actin.

Statistics

All experiments were performed at least in triplicate, and values are expressed as mean \pm SEM. Statistical significance ($P < 0.05$) was determined using Student's *t* test.

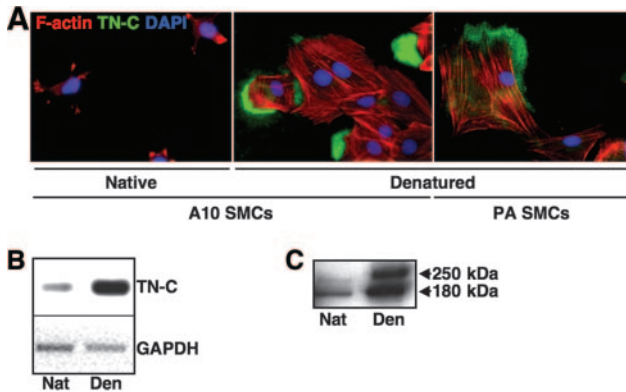


Figure 1. Adhesion-dependent induction of TN-C. A, A10 and PA SMCs cultivated on native or denatured type I collagen. F-Actin was stained with rhodamine phalloidin (red), whereas nuclei were visualized via DAPI (blue). An anti-TN-C antibody and a FITC-conjugated secondary antibody were used to detect TN-C (green). B, Semiquantitative RT-PCR for TN-C and GAPDH in SMCs cultured on native or denatured collagen. C, Western immunoblotting shows that expression of 250-kDa (upper band) and 180-kDa (lower band) TN-C isoforms increases in A10 SMCs cultured on denatured collagen, relative to the native version of this substrate.

An expanded Materials and Methods section is available in the online data supplement at <http://circres.ahajournals.org>.

Results

Adhesion-Dependent Induction of TN-C Coincides With Increased SMC Spreading

Previously, we established that induction of SMC TN-C is dependent on MMPs,¹⁴ which convert native, fibrillar type I collagen to a denatured, monomeric form that signals the production of TN-C at the transcriptional level.^{4,22} To determine whether adhesion-dependent induction of TN-C expression is accompanied by alterations in the F-actin cytoskeleton, A10 SMCs were cultivated either on native or denatured type I collagen and then examined for both F-actin and TN-C. A10 SMCs on native collagen adopted a spindle-shaped morphology, with F-actin-rich microspikes apparent at the cell periphery, as revealed by staining with rhodamine phalloidin (Figure 1A, left). SMCs with this appearance expressed low levels of TN-C mRNA and protein (Figure 1B and 1C), and they failed to deposit TN-C into their surrounding ECM (Figure 1A, left). In contrast, SMCs on denatured collagen spread extensively and possessed a well-developed F-actin stress fiber network (Figure 1A, middle). Under these conditions, SMCs expressed high levels of TN-C mRNA and protein (Figure 1B and 1C) and were surrounded by a TN-C-rich ECM (Figure 1A, middle). Importantly, primary adult rat PA SMCs behaved in an identical manner to A10 SMCs on native (Jones et al⁴ and not shown) and denatured collagen (Figure 1A, right). For all other studies, A10 SMCs were used as a model system, because their response to native and denatured type I collagen is identical to PA SMCs.^{4,22,27}

To quantify changes in cell shape that arise in response to changes in cell adhesion to type I collagen, SMCs were cultivated either on native or denatured collagen, before being visualized with Texas Red-C2 maleimide (Figure 2A, left and middle). Thereafter, individual SMCs were outlined, and the

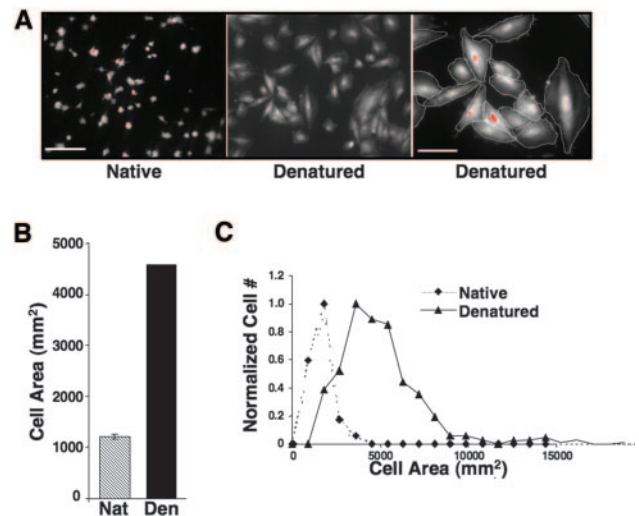


Figure 2. Quantifying cell spreading. A, SMCs cultured on native (left) or denatured (middle and right) collagen. Fluorescence microscopy was used to detect Texas Red maleimide-stained cells. Right, Magnified image of SMCs cultured on denatured collagen. White cell outlines were used to calculate cell surface area (shown at right). B, SHAPE analyses of cell areas for SMCs cultured either on native (hatched) or denatured (black) collagen. C, Distribution of cell area for SMCs cultivated on native (hatched line) or denatured (solid line) collagen.

area of each cell analyzed (Figure 2A, right). SHAPE analysis showed that the average area of SMCs cultured on denatured collagen was $\approx 4500 \mu\text{m}^2$, or ≈ 4 -fold larger than SMCs cultured on native collagen (Figure 2B). The population distribution of cell area for SMCs cultured on native or denatured collagen substrates was also determined (Figure 2C). Although this revealed that some overlap in SMC area exists between the smaller cells cultured on denatured collagen and the larger cells on native collagen, this quantitative assessment confirmed that cell area increases significantly when SMCs interact with denatured type I collagen. Collectively, these results indicate that increased TN-C expression in vascular SMCs cultured on denatured type I collagen is accompanied by acquisition of a prominent F-actin cytoskeleton and cell spreading.

TN-C Transcription Relies on Cytoskeletal Tension

Because formation of F-actin stress fibers and increased cell spreading leads to increases in cytoskeletal tension,²⁸ we next determined whether manipulating these parameters would affect TN-C transcription. To achieve this, TN1-GFP SMCs were used in which a full-length 4-kb TN-C gene promoter/GFP reporter construct was stably transfected into A10 cells.²⁷ TN1-GFP SMCs cultivated on denatured collagen were then treated with the actin-binding agent CCD, which reduced cell spreading (Figure 3A), and decreased TN-C gene promoter activity, as determined by Western immunoblotting for GFP (Figure 3B, top). Given that the activity of ERK1/2 MAPKs is suppressed and induced by native and denatured collagen, respectively,²² and because induction of SMC TN-C gene transcription on denatured collagen relies on activation of these effectors,²² we determined whether CCD-induced

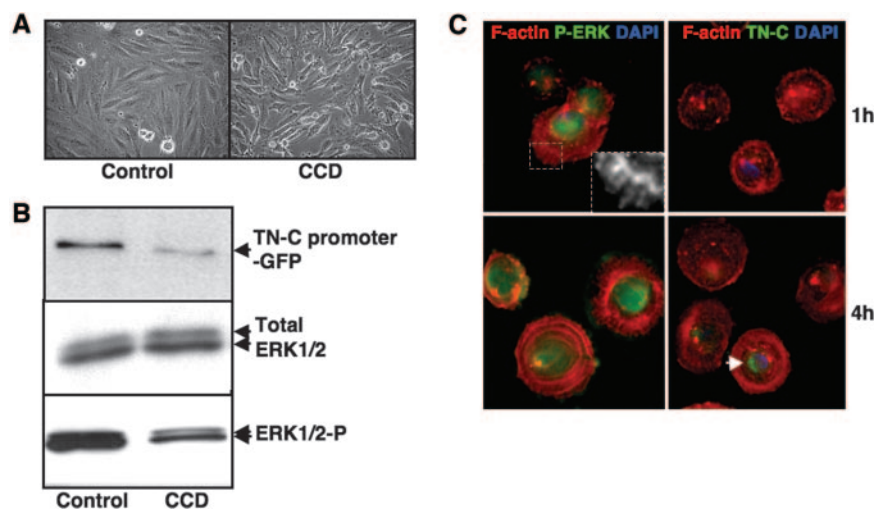


Figure 3. TN-C transcription, ERK1/2, and cytoskeletal architecture. A, TN1-GFP SMCs cultivated on denatured collagen with DMSO or CCD. B, Western immunoblotting shows that TN1-GFP cells on denatured collagen express GFP (at ≈ 31 kDa), an indication for TN-C transcription (top). Immunoblotting shows that CCD treatment does not affect total levels of ERK1/2 MAPKs (middle), yet activation of these upstream effectors is suppressed by CCD in TN1-GFP cells (bottom). C, Organization of F-actin (red) and expression of ERK1/2 (left panels, green) and TN-C (right panels, green) in SMCs plated on denatured collagen for 1 or 4 hours. DAPI (blue) identifies nuclei. Magnified inset (top left) shows that stress fibers form by 1 hour, preceding the appearance of TN-C in the ECM.

suppression of TN-C leads to reduced ERK1/2 activity in SMCs cultured on denatured collagen. Although total levels of nonphosphorylated ERK1/2 MAPK were unaffected by CCD (Figure 3B, middle), ERK1/2 activity was diminished by CCD (Figure 3B, bottom).

As already stated, activated ERK1/2 is required for TN-C transcription in A10 SMCs,²² and we have now shown that ERK1/2 activity appears to be dependent on F-actin stress fibers. Nevertheless, we wanted to define more precisely the sequence of morphological and signaling events culminating in appearance of TN-C in the ECM of SMCs cultured on denatured collagen. To achieve this, F-actin, activated ERK1/2, and TN-C were visualized in a time-course study using SMCs plated on denatured collagen for 1 and 4 hours. One hour after plating, F-actin stress fibers were evident within newly formed lamellipodia (Figure 3C, inset) and activated ERK1/2 was observed within cell nuclei (Figure 3C, top left), yet TN-C was not present in the surrounding ECM (Figure 3C, top right). By 4 hours, however, cell spreading had advanced, activated ERK1/2 remained in the nucleus (Figure 3C, bottom left), and extracellular TN-C was observed in the ECM (Figure 3C, bottom right). Thus, cell spreading and ERK1/2 activation precede the appearance of TN-C within the ECM in SMCs cultivated on denatured collagen.

Engineering SMC Shape to Control ERK1/2 Activity and TN-C Transcription

Because increases in cell spreading and cytoskeletal tension appear to control ERK1/2 and TN-C expression, we determined whether decreasing SMC spreading has the opposite effect. To achieve this, TN1-GFP SMCs were plated onto denatured collagen that had been overlaid with increasing concentrations of poly-HEME, a nonadhesive polymer that promotes cellular rounding (Figure 4A, top). As expected, rhodamine phalloidin staining for F-actin showed that as the concentration of poly-HEME increased, SMC spreading progressively decreased (Figure 4A, bottom). Consistent with their role as upstream regulators of SMC TN-C gene transcription,²² the activity of ERK1/2 MAPKs also declined, as cells became more rounded on increasing concentrations of

poly-HEME (Figure 4B). This reduction was not attributable to increased rates of apoptosis, evaluated by *in situ* staining of SMCs for annexin V (data not shown), or because of decreased availability of ERK1/2 MAPK substrates, as determined by Western immunoblotting (Figure 4C). In addition, Westerns for GFP, as a measure of TN-C gene promoter activity, showed that as SMC shape shifted from a spread to a more rounded phenotype, TN-C gene transcription also declined significantly (Figure 4D). Thus, reducing SMC spreading leads to decreased activation of activated ERK1/2 and one of its downstream targets, TN-C.

One question arising from the present study is whether any other components of the intracellular pathway leading to the induction of TN-C, besides ERK1/2 MAPKs, also rely on adhesion-dependent changes in F-actin. To address this, we evaluated expression of Prx2 in SMCs cultivated on native or denatured collagen. This homeobox gene transcription factor is coinduced and colocalizes with TN-C in hypertensive PAs, and it transactivates the TN-C gene promoter in SMCs.²⁷ Competitive RT-PCR showed that Prx2 mRNA expression was suppressed and induced by native and denatured collagen, respectively (Figure 5A). Therefore, like TN-C, Prx2 represents an ECM-responsive gene. Next, we determined whether Prx2 expression is also cell shape dependent. Cultivating SMCs on poly-HEME-coated denatured collagen plates revealed that the steady-state levels of Prx2 mRNA remained unchanged, regardless of whether cells were spread or round (Figure 5B). Consistent with this, treatment of SMCs cultivated on denatured collagen with CCD had no effect on Prx2 mRNA or protein expression (Figure 5C), despite the fact that CCD inhibited SMC spreading (Figure 3A). Thus, although Prx2 represents an ECM-responsive gene, its expression does not appear to require changes in SMC shape and cytoskeletal tension.

RhoA and ROCK Are Required for TN-C Expression

To begin to identify additional factors that control adhesion-dependent TN-C expression, we focused on RhoA and ROCK. RhoA is a multifunctional GTPase that is able to act as a mediator of adhesion-dependent signaling,²⁹ and it

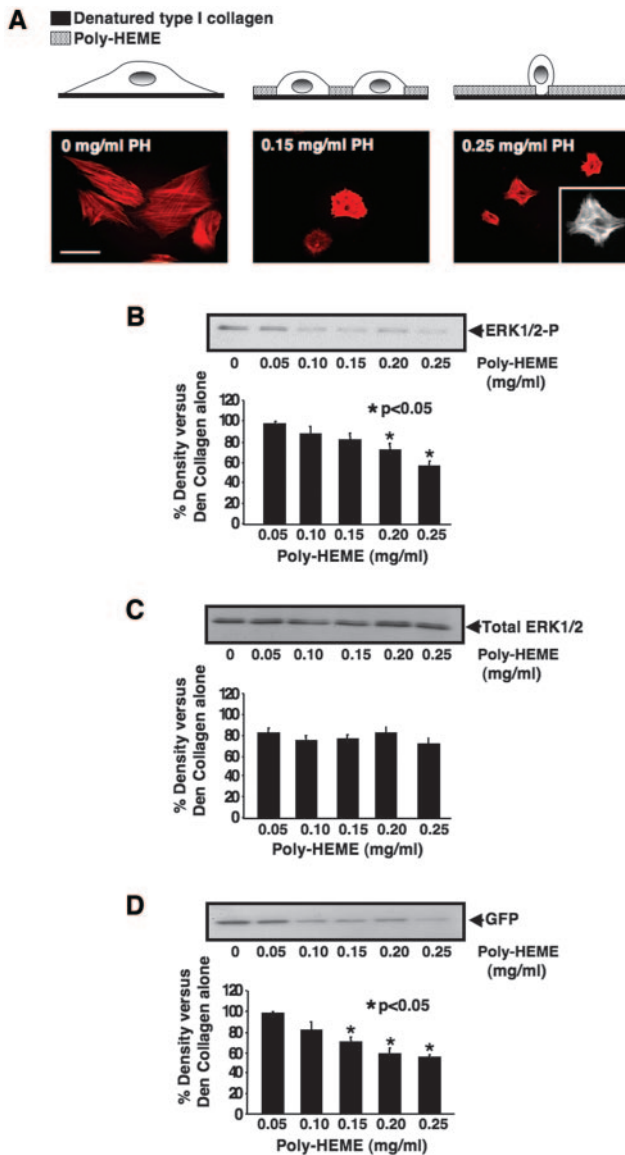


Figure 4. Changing vascular SMC shape controls ERK1/2 activity and TN-C transcription. A, Schematic (top) and rhodamine phalloidin-stained SMCs (bottom), showing anticipated and actual morphological effects of TN1-GFP cells cultured on denatured collagen, overlaid with increasing concentrations of poly-HEME. B, Western immunoblot for activated ERK1/2 in TN1-GFP cells plated on poly-HEME/denatured collagen substrates (top). Quantification of ERK1/2 protein levels by scanning densitometry (bottom). C, Western immunoblot for total ERK1/2 in TN1-GFP cells plated on poly-HEME/denatured collagen substrates (top). Quantification of total ERK1/2 (bottom). D, Western immunoblot for GFP in TN1-GFP cells plated on poly-HEME/denatured collagen substrates (top). Quantification of GFP levels (bottom).

controls cell shape and ERK1/2 MAPK activity.^{19,30} Moreover, ROCK, a downstream effector of activated RhoA, contributes to the pathobiology of systemic and pulmonary vascular disease, including MCT-induced pulmonary hypertension,^{26,31} the progression of which relies on TN-C.^{14,16}

Comparison of RhoA activity in SMCs maintained either on native or denatured collagen showed that the levels of activated RhoA were greater in SMCs on denatured collagen, whereas total levels of RhoA remained unchanged (Figure

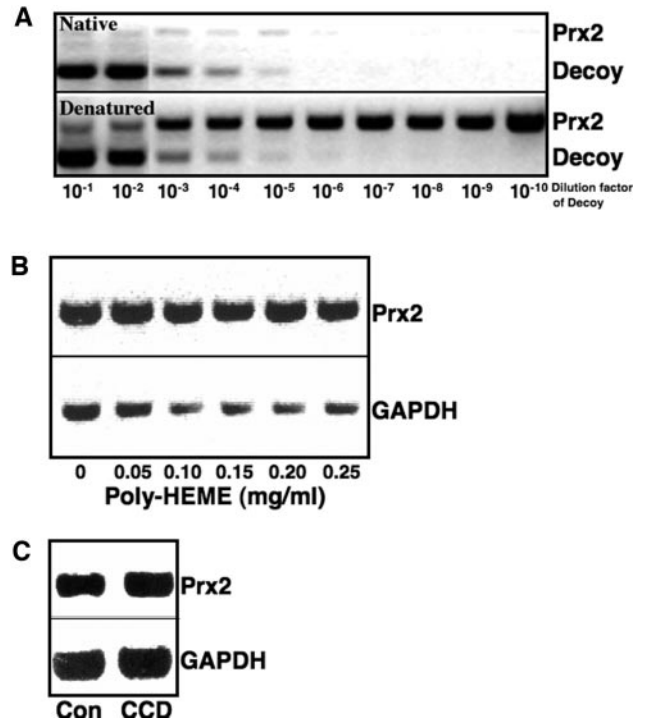


Figure 5. Effects of adhesion and shape on Prx2. A, Competitive PCR assays for Prx2 in SMCs cultured either on native or denatured collagen. B, Semiquantitative RT-PCR assay for Prx2 and GAPDH using total RNA isolated from A10 SMCs cultivated on denatured collagen, overlaid with different concentrations of poly-HEME. C, Semiquantitative RT-PCR assay for Prx2 and GAPDH in A10 SMCs cultivated on denatured collagen, treated either with DMSO, or with CCD.

6A). Next, to ascertain whether activated RhoA controls SMC shape and TN-C expression, SMCs were transiently transfected with a c-myc epitope-tagged dominant negative form of RhoA. SMCs expressing dominant negative RhoA lost their stress fibers, adopted a less spread morphology, and no longer expressed TN-C (Figure 6B). As well, studies were also conducted using a pharmacological inhibitor of Rho kinase (ROCK1, p160) Y27632, a downstream effector of RhoA.³¹ Rhodamine phalloidin of Y27632-treated SMCs cultured on denatured collagen showed that blockade of ROCK activity not only prevented stress fiber formation and cell spreading (Figure 6C) but that this was accompanied by a reduction of activated, nuclear ERK1/2, and decreased TN-C expression (Figure 6C). Collectively, these studies support the notion that changes in type I collagen structure control TN-C expression via activation of RhoA and ROCK.

Inhibiting ROCK Suppresses TN-C In Vivo

Finally, we determined whether our tissue culture studies were relevant in vivo. To achieve this, adult rats were injected with the alkaloid toxin MCT (which induces pulmonary arterial hypertension), with or without oral cotreatment with fasudil, another ROCK inhibitor.²⁶ A previous report has shown that fasudil prevents MCT-induced pulmonary arterial hypertension by improving endothelium-dependent relaxation and SMC hypercontraction,²⁶ yet its ability to control matrix production has not been examined. Fasudil treatment prevented increases in medial wall thickness that were evi-

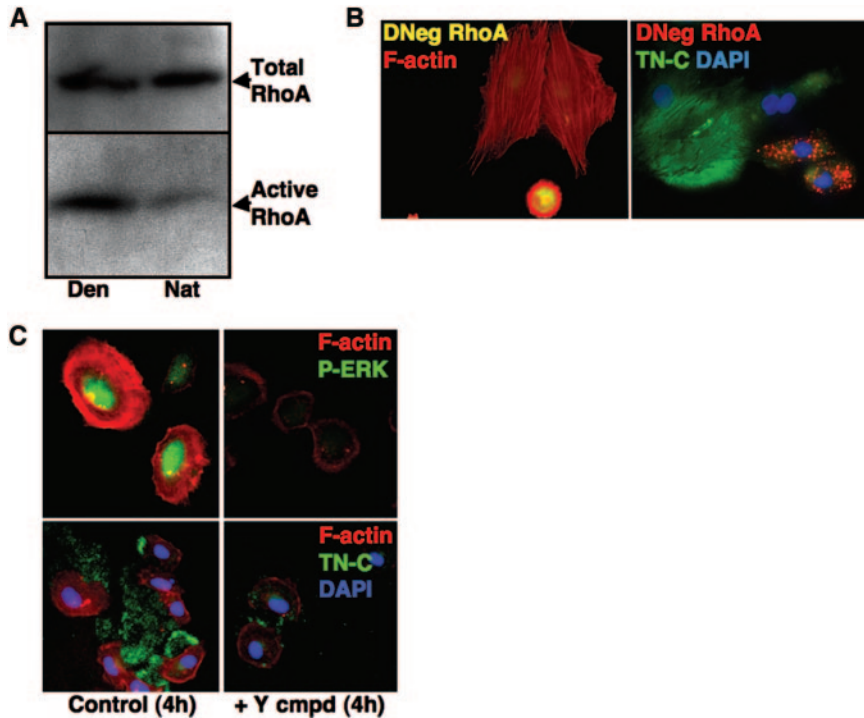


Figure 6. RhoA is required for TN-C expression. A, Pulldown and Western immunoblot studies to assess the levels of activated and total RhoA in A10 SMCs maintained either on native or denatured collagen. B, SMCs cultivated on denatured collagen following transfection with a dominant negative (DNeg) form of RhoA. Rhodamine phalloidin staining is in red, and DNeg RhoA is observed in green (left). On the right, TN-C is shown in green and dominant negative RhoA is red. C, Photomicrographs showing the effects of ROCK inhibition on F-actin (red), activated ERK1/2 (P-ERK) (green), and TN-C (green) in SMC cultivated on denatured collagen for 4 hours. DAPI reveals nuclei. H₂O served as a control for Y compound, a ROCK inhibitor.

dent in rats treated with MCT alone (Figure 7A). Moreover, immunohistochemistry showed that inhibiting ROCK reduced SMC TN-C expression in MCT-treated rat lungs, when compared with untreated control animals (Figure 7B).

Discussion

This study reveals that modifying the structure of type I collagen leads to RhoA/ROCK-dependent reorganization of the actin cytoskeleton and cell spreading. In turn, this newly acquired RhoA-dependent SMC phenotype is permissive for sustained ERK1/2 MAPK activity, which is required for TN-C gene transcription. Importantly, our tissue culture

experiments appear to be relevant in vivo, because inhibiting ROCK prevented SMC TN-C expression in an experimental model of pulmonary vascular disease. Moreover, because ROCK inhibition affects both vasoconstrictive responses,²⁶ and vascular remodeling at the level of the ECM, this study indicates that RhoA and ROCK may simultaneously control vasoconstriction and vascular remodeling (Figure 8).

ECM-directed changes in cell shape and cytoskeletal architecture are known to modify intracellular signaling pathways and gene expression events leading to distinct forms of cell and tissue behavior.^{32–37} A striking example of the profound effects that cell shape exerts on cell function has been provided by Chen and colleagues.²³ Using an ECM micropatterning technique to precisely control the degree of cell spreading, cell shape was identified as a key regulator human mesenchymal stem cell commitment to the osteoblast or adipocyte lineages.²³ Moreover, shape-dependent osteogenesis was shown to rely on RhoA. Because TN-C expression is dependent on both RhoA and cell spreading, at least in

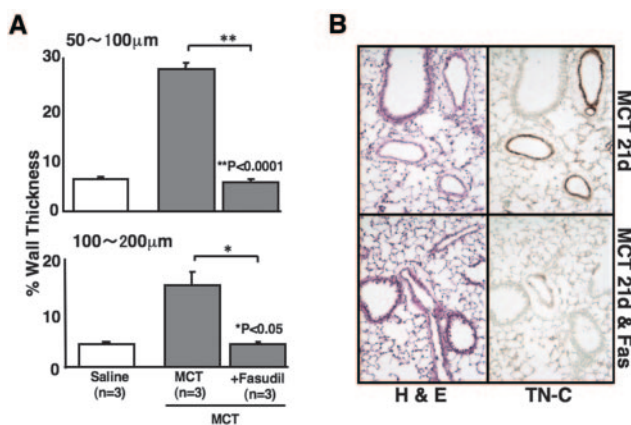


Figure 7. ROCK promotes TN-C expression in vivo. A, PA medial wall thickness in control, MCT, and fasudil-treated adult rats. Fasudil inhibits medial wall thickness in vessels of different sizes. B, Lung sections derived from MCT-treated rats at 21 days postinjection, either with or without coadministration of fasudil. Hematoxylin/eosin (H&E) staining and immunohistochemistry for TN-C (brown) reveal that fasudil blocks TN-C expression in MCT-treated rat lungs.

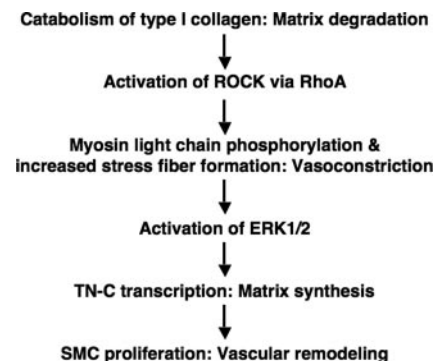


Figure 8. Hypothetical scheme showing how vasoconstriction and vascular remodeling may be coupled via ROCK.

SMCs, and TN-C is able to support differentiation of cultured osteoblast cells,³⁸ it is possible that commitment of human mesenchymal stem cells to the osteoblast lineage relies, in part, on shape-dependent induction of TN-C.

Our work and the work of others indicate that activation of RhoA in SMCs leads to a reactive pulmonary vascular SMC phenotype.^{26,31} However, evidence also exists showing that activation of RhoA supports expression of smooth muscle genes associated with the differentiated, quiescent state.³⁹ This difference may reflect inherent tissue-, region-, and developmental stage-specific differences between and within the pulmonary and systemic vascular systems.

One question arising from these studies is how do RhoA/ROCK-directed changes in cell morphology and the actin cytoskeleton lead to sustained activation of ERK1/2 and subsequently to an altered SMC transcriptional response? One possibility is that changes in F-actin spatially coordinate cell receptors and intracellular signaling mediators, thereby permitting upstream effectors, such as integrins and focal adhesion kinase (FAK), to couple with their downstream targets, which include ERK1/2 MAPKs. Another idea is that cell morphology may alter accessibility of ERK1/2 MAPKs to the nucleus. Indeed, exclusion of activated ERK1/2 from the nucleus has been shown to rely on the activation status of RhoA.⁴⁰ Thus, it is likely that cell shape permits appropriate interactions of upstream effectors with downstream mediators, such as ERK1/2, and that cell shape influences the interaction of these downstream mediators with their effectors.

Another way in which Rho GTPases and the cytoskeleton impact gene transcription has been described by Treisman and colleagues.⁴¹ In serum-starved cells, a myocardin-related protein known as MAL is predominantly localized to the cytoplasm, where it is sequestered by actin monomers. On serum stimulation, RhoA becomes active, and through its interaction with ROCK and mDia1, causes an accumulation of F-actin stress fibers and a decrease in the level of monomeric G actin. Consequently, MAL is released and translocates to the nucleus, where it associates with serum response factor (SRF), leading to activation of expression of SRF-dependent target genes.⁴¹ Whether this type of regulatory mechanism exists for TN-C is not yet known. However, it is worth pointing out that in our studies in which engineered SMC shape on poly-HEME-coated denatured collagen, stress fibers still formed in cells that were either spread or round. This suggests that it is cytoskeletal tension, afforded by denatured collagen and the F-actin cytoskeleton, rather than the polymerization state of actin, that controls ERK1/2-dependent TN-C transcription.

One drawback of our *in vivo* experiments is that they lack an important hemodynamic control, because fasudil may have both acute and chronic hemodynamic effects, and so it is not possible to determine from the *in vivo* studies whether the effects of fasudil on TN-C expression are attributable to direct ROCK inhibition in SMCs or are secondary to the hemodynamic effects of fasudil. This is noteworthy, especially because we have shown previously that TN-C expression is sensitive to pulmonary hemodynamics.⁸ Thus, it is possible that decreased TN-C expression may be achieved

both by a direct effect of fasudil and via an indirect hemodynamic effect. However, the fact that inhibiting ROCK activity in cultured SMCs also results in reduced TN-C expression indicates that the effects of this inhibition may be more direct.

Finally, this study raises the question as to whether Rho and ROCK simultaneously controls both vasoconstriction and vascular remodeling within hypertensive PAs. It is well established that the major regulatory mechanism of myosin/actin-based SMC contraction in hypertensive vessels involves phosphorylation and dephosphorylation of myosin light chain (MLC) by MLC kinase (MLCK) and MLC phosphatase (MLCP), respectively, and it has been shown that activated ROCK inhibits the activity of MLCP, thereby preventing dephosphorylation of MLC (reviewed by Loirand²⁵). In light of our results, such a ROCK/MLCK-dependent event would generate a cytoskeletal state that stimulates TN-C production. Thus, induction of the RhoA/ROCK pathway may coordinate both vasoconstriction and vascular remodeling in hypertensive vessels, thereby enhancing the therapeutic efficacy of ROCK inhibitors in the treatment of vascular diseases, including pulmonary hypertension.

Acknowledgments

We are extremely grateful to Dr Marlene Rabinovitch for providing tissue sections used in the preliminary phase of this study.

Sources of Funding

This work was supported by the following grants to P.L.J.: National Heart, Lung, and Blood Institute grant 1 R01 HL68798-01 and NIH grant P50 HL57144-06.

Disclosures

None.

References

1. Koyama H, Raines EW, Bornfeldt KE, Roberts JM, Ross R. Fibrillar collagen inhibits arterial smooth muscle proliferation through regulation of Cdk2 inhibitors. *Cell*. 1996;87:1069–1078.
2. Tanaka S, Koyama H, Ichii T, Shioi A, Hosoi M, Raines EW, Nishizawa Y. Fibrillar collagen regulation of plasminogen activator inhibitor-1 is involved in altered smooth muscle cell migration. *Arterioscler Thromb Vasc Biol*. 2002;22:1573–1578.
3. Franco CD, Hou G, Bendeck MP. Collagens, integrins, and the discoidin domain receptors in arterial occlusive disease. *Trends Cardiovasc Med*. 2002;12:143–148.
4. Jones PL, Crack J, Rabinovitch M. Regulation of tenascin-C, a vascular smooth muscle cell survival factor that interacts with the alpha v beta 3 integrin to promote epidermal growth factor receptor phosphorylation and growth. *J Cell Biol*. 1997;139:279–293.
5. Bendeck MP, Zempo N, Clowes AW, Galaray RE, Reidy MA. Smooth muscle cell migration and matrix metalloproteinase expression after arterial injury in the rat. *Circ Res*. 1994;75:539–545.
6. Jones PL, Rabinovitch M. Tenascin-C is induced with progressive pulmonary vascular disease in rats and is functionally related to increased smooth muscle cell proliferation. *Circ Res*. 1996;79:1131–1142.
7. Jones PL, Cowan KN, Rabinovitch M. Tenascin-C, proliferation and subendothelial fibronectin in progressive pulmonary vascular disease. *Am J Pathol*. 1997;150:1349–1360.
8. Jones PL, Chapados R, Baldwin HS, Raff GW, Vitvitsky EV, Spray TL, Gaynor JW. Altered hemodynamics controls matrix metalloproteinase activity and tenascin-C expression in neonatal pig lung. *Am J Physiol Lung Cell Mol Physiol*. 2002;282:L26–L35.
9. Ihida-Stansbury K, McKean DM, Gebb SA, Martin JF, Stevens T, Nemenoff R, Vaughn J, Lane K, Loyd J, Wheeler L, Morrell NW, Ivy D, Jones PL. Regulation and functions of the paired-related homeobox gene

- PRX1 in pulmonary vascular development and disease. *Chest*. 2005;128(6 suppl):591S.
10. Ivy DD, McMurtry IF, Colvin K, Imamura M, Oka M, Lee DS, Gebb S, Jones PL. Development of occlusive neointimal lesions in distal pulmonary arteries of endothelin B receptor-deficient rats: a new model of severe pulmonary arterial hypertension. *Circulation*. 2005;111:2988–2996.
 11. Yamamoto K, Onoda K, Sawada Y, Fujinaga K, Imanaka-Yoshida K, Shimpo H, Yoshida T, Yada I. Tenascin-C is an essential factor for neointimal hyperplasia after aortotomy in mice. *Cardiovasc Res*. 2005;65:737–742.
 12. Imanaka-Yoshida K, Matsuura R, Isaka N, Nakano T, Sakakura T, Yoshida T. Serial extracellular matrix changes in neointimal lesions of human coronary artery after percutaneous transluminal coronary angioplasty: clinical significance of early tenascin-C expression. *Virchows Arch*. 2001;439:185–190.
 13. Wallner K, Li C, Shah PK, Fishbein MC, Forrester JS, Kaul S, Sharifi BG. Tenascin-C is expressed in macrophage-rich human coronary atherosclerotic plaque. *Circulation*. 1999;99:1284–1289.
 14. Cowan KN, Jones PL, Rabinovitch M. Elastase and matrix metalloproteinase inhibitors induce regression, and tenascin-C antisense prevents progression, of vascular disease. *J Clin Invest*. 2000;105:21–34.
 15. Jones FS, Jones PL. The tenascin family of ECM glycoproteins: structure, function, and regulation during embryonic development and tissue remodeling. *Dev Dyn*. 2000;218:235–259.
 16. Cowan KN, Jones PL, Rabinovitch M. Regression of hypertrophied rat pulmonary arteries in organ culture is associated with suppression of proteolytic activity, inhibition of tenascin-C, and smooth muscle cell apoptosis. *Circ Res*. 1999;84:1223–1233.
 17. Reardon DA, Akabani G, Coleman RE, Friedman AH, Friedman HS, Herndon JE 2nd, McLendon RE, Pegram CN, Provenzale JM, Quinn JA, Rich JN, Vredenburg JJ, Desjardins A, Gururangan S, Badrudoja M, Dowell JM, Wong TZ, Zhao XG, Zalutsky MR, Bigner DD. Salvage radioimmunotherapy with murine iodine-131-labeled antitenascin monoclonal antibody 81C6 for patients with recurrent primary and metastatic malignant brain tumors: phase II study results. *J Clin Oncol*. 2006;24:115–122.
 18. Rizzieri DA, Akabani G, Zalutsky MR, Coleman RE, Metzler SD, Bowsher JE, Toaso B, Anderson E, Lagoo A, Clayton S, Pegram CN, Moore JO, Gockerman JP, DeCastro C, Gasparetto C, Chao NJ, Bigner DD. Phase I trial study of 131I-labeled chimeric 81C6 monoclonal antibody for the treatment of patients with non-Hodgkin lymphoma. *Blood*. 2004;104:642–648.
 19. Aso N, Tamura A, Nasu M. Circulating tenascin-C levels in patients with idiopathic dilated cardiomyopathy. *Am J Cardiol*. 2004;94:1468–1470.
 20. Bailey M, Pillarisetti S, Jones P, Xiao H, Simionescu D, Vyavahare N. Involvement of matrix metalloproteinases and tenascin-C in elastin calcification. *Cardiovasc Pathol*. 2004;13:146–155.
 21. Thomasset N, Lochter A, Sympton CJ, Lund LR, Williams DR, Behrendtsen O, Werb Z, Bissell MJ. Expression of autoactivated stromelysin-1 in mammary glands of transgenic mice leads to a reactive stroma during early development. *Am J Pathol*. 1998;153:457–467.
 22. Jones PL, Jones FS, Zhou B, Rabinovitch M. Induction of vascular smooth muscle cell tenascin-C gene expression by denatured type I collagen is dependent upon a beta3 integrin-mediated mitogen-activated protein kinase pathway and a 122-base pair promoter element. *J Cell Sci*. 1999;112(pt 4):435–445.
 23. McBeath R, Pirone DM, Nelson CM, Bhadriraju K, Chen CS. Cell shape, cytoskeletal tension, and RhoA regulate stem cell lineage commitment. *Dev Cell*. 2004;6:483–495.
 24. Paszek MJ, Zahir N, Johnson KR, Lakins JN, Rozenberg GI, Gefen A, Reinhart-King CA, Margulies SS, Dembo M, Boettiger D, Hammer DA, Weaver VM. Tensional homeostasis and the malignant phenotype. *Cancer Cell*. 2005;8:241–254.
 25. Loirand G, Guerin P, Pacaud P. Rho kinases in cardiovascular physiology and pathophysiology. *Circ Res*. 2006;98:322–334.
 26. Abe K, Shimokawa H, Morikawa K, Uwatoku T, Oi K, Matsumoto Y, Hattori T, Nakashima Y, Kaibuchi K, Sueishi K, Takeshit A. Long-term treatment with a Rho-kinase inhibitor improves monocrotaline-induced fatal pulmonary hypertension in rats. *Circ Res*. 2004;94:385–393.
 27. Jones FS, Meech R, Edelman DB, Oakey RJ, Jones PL. Prx1 controls vascular smooth muscle cell proliferation and tenascin-C expression and is upregulated with Prx2 in pulmonary vascular disease. *Circ Res*. 2001;89:131–138.
 28. Wang N, Naruse K, Stamenovic D, Fredberg JJ, Mijailovich SM, Tolic-Norrelykke IM, Polte T, Mannix R, Ingber DE. Mechanical behavior in living cells consistent with the tensegrity model. *Proc Natl Acad Sci U S A*. 2001;98:7765–7770.
 29. Ridley A. Rho GTPases. Integrating integrin signaling. *J Cell Biol*. 2000;150:F107–F109.
 30. Allen WE, Jones GE, Pollard JW, Ridley AJ. Rho, Rac and Cdc42 regulate actin organization and cell adhesion in macrophages. *J Cell Sci*. 1997;110(pt 6):707–720.
 31. Fagan KA, Oka M, Bauer NR, Gebb SA, Ivy DD, Morris KG, McMurtry IF. Attenuation of acute hypoxic pulmonary vasoconstriction and hypoxic pulmonary hypertension in mice by inhibition of Rho-kinase. *Am J Physiol Lung Cell Mol Physiol*. 2004;287:656–664.
 32. Chen CS, Mrksich M, Huang S, Whitesides GM, Ingber DE. Geometric control of cell life and death. *Science*. 1997;276:1425–1428.
 33. Roskelley CD, Desprez PY, Bissell MJ. Extracellular matrix-dependent tissue-specific gene expression in mammary epithelial cells requires both physical and biochemical signal transduction. *Proc Natl Acad Sci U S A*. 1994;91:12378–12382.
 34. Boudreau NJ, Jones PL. Extracellular matrix and integrin signalling: the shape of things to come. *Biochem J*. 1999;339(pt 3):481–488.
 35. Weaver VM, Petersen OW, Wang F, Larabell CA, Briand P, Damsky C, Bissell MJ. Reversion of the malignant phenotype of human breast cells in three-dimensional culture and in vivo by integrin blocking antibodies. *J Cell Biol*. 1997;137:231–245.
 36. Folkman J, Haudenschild CC, Zetter BR. Long-term culture of capillary endothelial cells. *Proc Natl Acad Sci U S A*. 1979;76:5217–5221.
 37. Huang S, Chen CS, Ingber DE. Control of cyclin D1, p27(Kip1), and cell cycle progression in human capillary endothelial cells by cell shape and cytoskeletal tension. *Mol Biol Cell*. 1998;9:3179–3193.
 38. Mackie EJ, Ramsey S. Modulation of osteoblast behaviour by tenascin. *J Cell Sci*. 1996;109(pt 6):1597–1604.
 39. Mack CP, Somlyo AV, Hautmann M, Somlyo AP, Owens GK. Smooth muscle differentiation marker gene expression is regulated by RhoA-mediated actin polymerization. *J Biol Chem*. 2001;276:341–347.
 40. Zuckerbraun BS, Shapiro RA, Billiar TR, Tzeng E. RhoA influences the nuclear localization of extracellular signal-regulated kinases to modulate p21Waf/Cip1 expression. *Circulation*. 2003;108:876–881.
 41. Miralles F, Posern G, Zaromytidou AI, Treisman R. Actin dynamics control SRF activity by regulation of its coactivator MAL. *Cell*. 2003;113:329–342.

Circulation Research

JOURNAL OF THE AMERICAN HEART ASSOCIATION



ROCK Controls Matrix Synthesis in Vascular Smooth Muscle Cells: Coupling Vasoconstriction to Vascular Remodeling

Rene Chapados, Khotaro Abe, Kaori Ihida-Stansbury, David McKean, Adam T. Gates, Michael Kern, Sandra Merklinger, John Elliott, Anne Plant, Hiroaki Shimokawa and Peter Lloyd Jones

Circ Res. 2006;99:837-844; originally published online September 21, 2006;

doi: 10.1161/01.RES.0000246172.77441.f1

Circulation Research is published by the American Heart Association, 7272 Greenville Avenue, Dallas, TX 75231

Copyright © 2006 American Heart Association, Inc. All rights reserved.

Print ISSN: 0009-7330. Online ISSN: 1524-4571

The online version of this article, along with updated information and services, is located on the
World Wide Web at:

<http://circres.ahajournals.org/content/99/8/837>

Data Supplement (unedited) at:

<http://circres.ahajournals.org/content/suppl/2006/09/21/01.RES.0000246172.77441.f1.DC1>

Permissions: Requests for permissions to reproduce figures, tables, or portions of articles originally published in *Circulation Research* can be obtained via RightsLink, a service of the Copyright Clearance Center, not the Editorial Office. Once the online version of the published article for which permission is being requested is located, click Request Permissions in the middle column of the Web page under Services. Further information about this process is available in the [Permissions and Rights Question and Answer](#) document.

Reprints: Information about reprints can be found online at:
<http://www.lww.com/reprints>

Subscriptions: Information about subscribing to *Circulation Research* is online at:
<http://circres.ahajournals.org/subscriptions/>

Materials and Methods

Animals

Lungs were harvested from adult male Sprague-Dawley rats, 14, 21 and 28 days after injection of MCT or saline. Lungs and heart tissue was fixed and processed as described^{1, 2}. For fasudil (a ROCK inhibitor) experiments, adult rats were injected with MCT, with or without concomitant oral treatment of 100mg/kg per day of fasudil as described previously³. Right ventricular hypertrophy and medial wall thickness were assessed as described¹.

Histochemical analyses

Anti-TN-C rabbit polyclonal antibody diluted in PBSA was applied to sections overnight at 4°C. Immunohistochemical detection was achieved using horseradish peroxidase-conjugated secondary antibodies. To visualize TN-C, sections were exposed to diaminobenzidine, prior to counterstaining with hemotoxylin. Serial sections were exposed to hemotoxylin and eosin stains.

Cell culture

Vascular SMCs were routinely maintained in Medium 199 (M199) containing 10% fetal bovine serum. Assessment of TN-C gene promoter activity was determined using A10 TN1-GFP SMCs. Native and denatured type I collagen substrates were prepared based on our published methods². For inhibition of F-actin polymerization, SMCs were treated with 1 μ M cytochalasin D (CCD), or with DMSO as a control. For inhibition of MEK1 or ROCK, cultures were supplemented with 50 μ m PD98059 (DMSO as a

control) or 30 μ M of Y27632 (H₂O as a control) respectively. For these experiments, cells were maintained in M199 plus 2% FBS.

Immuno/cytochemistry

For detection of F-actin, TN-C and ERK1/2, SMCs were fixed in 4% paraformaldehyde/PBS, permeabilized in 0.1% Triton-X 100, rinsed in PBS and then blocked in PBS supplemented with PBSA and 10% normal goat serum. Cells were then incubated overnight at 4°C with rabbit polyclonal antisera against TN-C (Chemicon) or activated ERK1/2 (Cell Signaling), or with a mouse monoclonal antibody against human c-myc (Sigma). Cells were rinsed in PBS, and incubated with a FITC-conjugated goat anti-rabbit IgG. For F-actin, cells were incubated with Alexa Fluor 594 phalloidin in PBS. Slides were mounted using Antifade reagent containing DAPI for detection of nuclei. Observations and photomicrographs were obtained using epifluorescence.

Semi-quantitative & competitive RT-PCR

Poly(A⁺) RNA was reverse transcribed using first strand cDNA synthesis. Semi quantitative RT-PCR reactions were performed with cDNAs generated from cells cultivated on native and denatured collagen, or on poly-HEME substrates using the following primers; TN-C (forward 5'-GCTCTCGATGGTCCATCTGGC-3' & reverse 5'-TCGTAGCAGTGGTAGAACTC-3'), Prx2 (forward 5'-ATGGCAGTGCCAAACGG-3' and reverse 5'-GTTGCAGGACTTGAACCTCC-3'), and GAPDH (forward 5'-TGGGGCCAAAAGGGTCATCATCTC-3' & reverse 5'-GCCGCCTGCTTCACCACCTTCTT-3'). For competitive PCR, an internal decoy

competitor cDNA for Prx2 was generated that was distinguishable (i.e. smaller) from the full-length Prx2 cDNA. The following primer pair was used: Prx2 (forward: 5´- GGA ATT CGA CAG CGC GGC CGC CGC CTT -3´; reverse: 5´-AGG ACT TGA ACC TCC ACT TGA GCA GCG AGG CAG AGC-3´). The concentration of decoy was adjusted to 100 ng/ml, and thereafter serially diluted to produce a known range of DNA concentrations (10^{-1} - 10^{-10}). Diluted decoy was then be added to a known amount (2.5 ng/ml) of cDNA. Final PCR reactions were carried out using primers designed for the semi-quantitative PCR studies. After completion of reactions, equal aliquots of each sample were resolved on agarose gels and visualized by ethidium bromide staining.

Western immunoblotting

SMCs were lysed in RIPA buffer. Samples were quantified and equal amounts of protein were separated on 4-15% SDS-PAGE gels. Proteins were transferred to PVDF membranes, and were blocked in wash buffer supplemented with 5% non-fat milk. Membranes were also incubated with a rabbit polyclonal anti-TN-C antibody or with an anti-GFP mouse monoclonal antibody respectively. To detect ERK1/2 MAPKs, membranes were incubated with antibodies against total ERK1/2, or phosphorylated ERK1/2, and species-specific peroxidase-conjugated secondary antisera. Thereafter, TN-C, GFP and ERK1/2 proteins were visualized by ECL, before exposure to Kodak X-Omat film. In some instances, immunoblots were quantified by densitometry and standardized as a percent of the control.

Cell SHAPE analysis

Cells were rinsed with PBS and permeabilized with 0.1% TX-100 in PBS for 5 min at RT, before being stained with Texas Red maleimide. Samples were imaged on a Zeiss Axiovert S100 TV inverted microscope. An outline of each cell in a frame was drawn manually using Innovision image-processing software. Cells were outlined, and the region of interest line was typically drawn through the middle of smaller processes. The shape of each cell was analyzed through the SHAPE module of the software package. Data for total area was then determined.

Poly-HEME experiments

SMCs were plated on increasing concentrations of the non-adhesive substrate poly (2-hydroxyethylmethacrylate) or poly-HEME. Poly-HEME was dissolved in 95% v/v ethanol to give final concentrations of 0.05, 0.10, 0.15, 0.20 and 0.25 mg/mL. Prior to plating poly-HEME, tissue culture plates were pre-coated with denatured collagen. Surfaces were equilibrated for 3 h with serum free M199, prior to plating and culturing cells for 24 h.

Rho pulldown assays

SMCs cultured either on native or denatured collagen were released from substrates and lysed in 1 x MLB buffer (Upstate Biotechnology), and then centrifuged at 14K g for 5 min. 20 µg of protein was analyzed via western immunoblotting for total RhoA using standard techniques and an anti-RhoA antibody (Santa Cruz). In parallel, equal amounts of protein (300 µg) within MLB lysates in 0.5 ml total volume were treated with

40 μ l Rhotekin Rho binding domain-agarose beads (Upstate Biotechnology). After 45 min incubation at 4°C beads were collected by centrifugation, washed and resuspended in 2 x Laemmli buffer. Supernatants were resolved via SDS-PAGE and active RhoA released from beads was assessed by western immunoblotting as described above.

Cellular transfection studies

Transient transfection experiments were performed using a total of 3 μ g of DNA and Lipofectamine. The following plasmid constructs were used: pcDNA3.1(-)/RhoA-N19-myc (dominant negative RhoA). Cells were incubated in the presence of DNA-Lipofectamine for 4 h at which time the antibiotic-free M199 containing DNA-Lipofectamine complexes was replaced with antibiotic-free M199 containing 2% FBS. Cells were replated at 48 h post-transfection onto denatured collagen substrates, prior to fixation and evaluation of c-myc, TN-C and F-actin via immuno/cytochemistry.

Annexin V staining

A10 TN1-GFP SMCs were cultured for 24 h on differing concentrations of poly-HEME. The cells were rinsed with PBS and stained for Annexin V using the Apoalert Annexin V Apoptosis kit, and then counterstained with DAPI for detection of total nuclei. The % of apoptotic cells was directly visualized by epifluorescence (n=500 total cells).

Statistics

All experiments were performed at least in triplicate and values are expressed as mean \pm SEM. Statistical significance ($p < 0.05$) was determined using Student's t-test.

1. Jones PL, Rabinovitch M. Tenascin-C is induced with progressive pulmonary vascular disease in rats and is functionally related to increased smooth muscle cell proliferation. *Circ Res.* 1996; 79:1131-1142.
2. Jones FS, Meech R, Edelman DB, Oakey RJ, Jones PL. Prx1 controls vascular smooth muscle cell proliferation and tenascin-C expression and is upregulated with Prx2 in pulmonary vascular disease. *Circ Res.* 2001; 89:131-138.
3. Abe K, Shimokawa H, Morikawa K, Uwatoku T, Oi K, Matsumoto Y, Hattori T, Nakashima Y, Kaibuchi K, Sueishi K, Takeshit A. Long-term treatment with a Rho-kinase inhibitor improves monocrotaline-induced fatal pulmonary hypertension in rats. *Circ Res.* 2004; 94:385-393.